Annals of the Academy of Romanian Scientists
Series on Physics and Chemistry Sciences
ISSN 2559-1061 Volume 3, Number 1/2018

QUASIPARTICLE VIBRATION COUPLING EFFECTS ON GAMOW-TELLER RESPONSE IN SUPERFLUID NUCLEI

Y.F. Niu*

Abstract

Gamow-Teller (GT) excitation is one of the most important spin-isospin modes in nuclei. The commonly used quasiparticle random phase approximation (QRPA) model cannot describe the width and detailed fragmentation of GT strength distribution. In order to overcome this limit, the quasiparticle vibration coupling (QPVC) is included on top of the QRPA model. The subtraction method is applied in the QPVC calculation to avoid double counting problem. The QPVC effects on GT excitation in ^{120}Sn are discussed. With the inclusion of QPVC, a width is developed and the experimental data of GT response in the giant resonance region is well reproduced.

keywords: Gamow-Teller excitation, Quasiparticle random phase approximation, Quasiparticle vibration coupling

*nyfster@gmail.com ELI-NP, Horia Hulubei National Institute for Physics and Nuclear Engineering, 30 Reactorului Street, RO-077125 Bucharest-Magurele, Romania

1 Introduction

Gamow-Teller (GT) excitation is one of the most important spin-isospin excitation modes in nuclei [1]. It involves two basic degrees of freedom in nuclei, spin and isospin, therefore it can provide useful information on the spin-isopin channel of the nuclear effective interaction. It is also the dominant transition in nuclear weak interaction processes [2, 3], like β decay [4], electron capture [5, 6] and neutrino-nucleus scattering [7, 8], which play important roles in astrophysical processes such as rapid neutron capture process, supernova explosion and so on.

The GT resonances (GTR) have been studied both experimentally and theoretically. In experiment, one can use (p,n) or (^{3}He,t) reaction to excite GTR modes [9, 10]. From the cross section of these reactions, the strength function of GT can be extracted. In theory, the shell model and random phase approximation (RPA) are the most commonly used microscopic models. Compared to shell model, which can only be limited to calculate nuclei up to mass number 60 or around magic ones, the RPA model could be applied to the calculations of the whole nuclear chart. The basic idea of the RPA model is that giant resonances are considered as the superposition of many 1 particle-1 hole (1p-1h) excitations. This consideration of 1p-1h configuration space simplifies the calculation and makes it possible to include the configuration space up to a high energy. RPA could give a good description of the centroid energy of GTR [11, 12]. However, the width and detailed fragmentation of giant resonances cannot be described. The width of giant resonances is caused by the coupling of 1p-1h configurations with more complicated configurations like 2p-2h etc. So, in order to describe the width, one needs to go beyond RPA and include more complicated configurations. A direct way is to include both 1p-1h and 2p-2h configurations in the model space, which is called the second RPA (SRPA) [13]. An alternative way is to include the 1p-1h and 1p-1h coupled with phonons (1p-1h $\otimes$ 1 phonon) in the model space, which is called RPA + particle-vibration coupling (PVC) model [14]. The advantage of this method is that the calculation is simplified compared to the SRPA approach, yet it still keeps the main feature of SRPA.

In recent years, the self-consistent RPA+PVC model has been developed based on both relativistic and Skyrme density functionals. It has been successfully applied to the calculations of giant and pygmy resonances [15, 16, 17], spin-isospin excitations[18, 19, 20], and even β-decay processes [21]. In the RPA+PVC approach, the pairing correlations were not considered. In order to describe the superfluid nuclei, the pairing correlations were further included, and therefore the quasiparticle RPA (QRPA) + quasiparticle vibration coupling (QPVC) model has also been developed with relativistic and Skyrme density functionals [22]. In this work, we will briefly review the quasiparticle vibration coupling effects on the GT excitations in superfluid nuclei based on the Skyrme density functional.

2 Formulas

The QRPA+QPVC equation reads

$$\begin{pmatrix} \mathcal{D}+\mathcal{A}_1(E) & \mathcal{A}_2(E) \\ -\mathcal{A}_3(E) & -\mathcal{D}-\mathcal{A}_4(E) \end{pmatrix} \begin{pmatrix} F^{(\nu)} \\ \bar{F}^{(\nu)} \end{pmatrix} = (\Omega_\nu - i\frac{\Gamma_\nu}{2}) \begin{pmatrix} F^{(\nu)} \\ \bar{F}^{(\nu)} \end{pmatrix}. \tag{2.1}$$

$\mathcal{D}$ is a diagonal matrix containing the physical QRPA eigenvalues. The $\mathcal{A}_i$ matrices are complex and energy dependent, associated with the coupling to the doorway states. The expressions of $\mathcal{A}_i$ in the QRPA basis $|n\rangle$ are given by

$$(\mathcal{A}_1)_{mn} = \sum_{ab,a'b'} W^{\downarrow}_{ab,a'b'}(E) X^{(m)}_{ab} X^{(n)}_{a'b'} + W^{\downarrow *}_{ab,a'b'}(-E) Y^{(m)}_{ab} Y^{(n)}_{a'b'}, \tag{2.2}$$

$$(\mathcal{A}_2)_{mn} = \sum_{ab,a'b'} W^{\downarrow}_{ab,a'b'}(E) X^{(m)}_{ab} Y^{(n)}_{a'b'} + W^{\downarrow *}_{ab,a'b'}(-E) Y^{(m)}_{ab} X^{(n)}_{a'b'}, \tag{2.3}$$

$$(\mathcal{A}_3)_{mn} = \sum_{ab,a'b'} W^{\downarrow}_{ab,a'b'}(E) Y^{(m)}_{ab} X^{(n)}_{a'b'} + W^{\downarrow *}_{ph,p'h'}(-E) X^{(m)}_{ab} Y^{(n)}_{a'b'}, \tag{2.4}$$

$$(\mathcal{A}_4)_{mn} = \sum_{ab,a'b'} W^{\downarrow}_{ab,a'b'}(E) Y^{(m)}_{ab} Y^{(n)}_{a'b'} + W^{\downarrow *}_{ab,a'b'}(-E) X^{(m)}_{ab} X^{(n)}_{a'b'}. \tag{2.5}$$

$X^{(n)}_{ab}$ and $Y^{(n)}_{ab}$ are the forward-going and backward-going amplitudes associated with the QRPA eigenstates $|n\rangle$, respectively. The detailed QRPA calculation can be found in Ref. [23]. Here and in what follows, the indices a, b label the so-called BCS quasi-particle states in the canonical bases, that are those defined by the operators α and $\alpha^\dagger$ at p. 248 of Ref. [24].

The spreading matrix $W^{\downarrow}_{ab,a'b'}(E)$ is the most important quantity in the QRPA+QPVC model,

$$W^{\downarrow}_{ab,a'b'} = \langle ab|V\frac{1}{E-\hat{H}}V|a'b'\rangle = \sum_{NN'} \langle ab|V|N\rangle\langle N|\frac{1}{E-\hat{H}}|N'\rangle\langle N'|V|a'b'\rangle, \tag{2.6}$$

where $|N\rangle = |a''b''\rangle \otimes |nL\rangle$ represents a doorway state and a'', b'' are BCS quasi-particle states, as recalled above. The doorway states are made of a two BCS quasi-particle excitation $|ab\rangle$ coupled to a collective vibration $|nL\rangle$ of angular momentum L and energy ω_{nL}. The properties of these collective vibrations, i.e., phonons $|nL\rangle$, are obtained by computing the QRPA response with the same Skyrme interaction, for states of natural parity $L^\pi = 0^+$, 1^-, 2^+, 3^-, 4^+, 5^-, and 6^+. We have retained the phonons with energy less than 20 MeV and absorbing a fraction of the non-energy weighted isoscalar or isovector sum rule (NEWSR) strength larger than 5%.

The final expression for spreading matrix in angular momentum coupled form $W^{\downarrow J}_{ab,a'b'}$ reads

$$W^{\downarrow J}_{1ab,a'b'} = \delta_{j_b j_{b'}} \delta_{l_b l_{b'}} \delta_{j_a j_{a'}} \frac{1}{\hat{j}_a^2} \sum_{a''a'''\tilde{a}''\tilde{b}''} \sum_{nL} \delta_{j_{a''} j_{a'''}} \delta_{l_{a''} l_{a'''}}$$

$$\frac{\langle a||V||a'',nL\rangle C_{a''\tilde{a}''}C_{b\tilde{b}''}C^{\dagger}_{\tilde{a}''a'''}C^{\dagger}_{\tilde{b}''b'}\langle a'||V||a''',nL\rangle}{E-[E_{\tilde{a}''}+E_{\tilde{b}''}+\omega_{nL}\pm(\lambda_n-\lambda_p)]+i\Delta}, \tag{2.7}$$

$$W^{\downarrow J}_{2ab,a'b'} = \delta_{j_a j_{a'}}\delta_{l_a l_{a'}}\delta_{j_b j_{b'}}\frac{1}{\hat{j}_b^2}\sum_{b''b'''\tilde{a}''\tilde{b}''}\sum_{nL}\delta_{j_{b''}j_{b'''}}\delta_{l_{b''}l_{b'''}}$$

$$\frac{\langle b||V||b'',nL\rangle C_{a\tilde{a}''}C_{b''\tilde{b}''}C^{\dagger}_{\tilde{a}''a'}C^{\dagger}_{\tilde{b}''b'''}\langle b'||V||b''',nL\rangle}{E-[E_{\tilde{a}''}+E_{\tilde{b}''}+\omega_{nL}\pm(\lambda_n-\lambda_p)]+i\Delta}, \tag{2.8}$$

$$W^{\downarrow J}_{3ab,a'b'} = (-)^{j_a+j_b+J}\left\{\begin{array}{ccc} j_a & j_b & J \\ j_{b'} & j_{a'} & L\end{array}\right\}\sum_{a'''b''\tilde{a}''\tilde{b}''}\sum_{nL}\delta_{j_{b''}j_{b'}}\delta_{l_{b''}l_{b'}}\delta_{j_{a'''}j_a}\delta_{l_{a'''}l_a}$$

$$\frac{\langle b||V||b'',nL\rangle C_{a\tilde{a}''}C_{b''\tilde{b}''}C^{\dagger}_{\tilde{a}''a'''}C^{\dagger}_{\tilde{b}''b'}\langle a'||V||a''',nL\rangle}{E-[E_{\tilde{a}''}+E_{\tilde{b}''}+\omega_{nL}\pm(\lambda_n-\lambda_p)]+i\Delta}, \tag{2.9}$$

$$W^{\downarrow J}_{4ab,a'b'} = (-)^{j_{a'}+j_{b'}+J}\left\{\begin{array}{ccc} j_{a'} & j_{b'} & J \\ j_b & j_a & L\end{array}\right\}\sum_{b'''a''\tilde{a}''\tilde{b}''}\sum_{nL}\delta_{j_{a''}j_{a'}}\delta_{l_{a''}l_{a'}}\delta_{j_{b'''}j_b}\delta_{l_{b'''}l_b}$$

$$\frac{\langle a||V||a'',nL\rangle C_{b\tilde{b}''}C_{a''\tilde{a}''}C^{\dagger}_{\tilde{b}''b'''}C^{\dagger}_{\tilde{a}''a'}\langle b'||V||b''',nL\rangle}{E-[E_{\tilde{a}''}+E_{\tilde{b}''}+\omega_{nL}\pm(\lambda_n-\lambda_p)]+i\Delta}. \tag{2.10}$$

In the above formulas, $\hat{j}_i^2$ is a shorthand notation for $2j_i+1$. C represents the unitary transformation matrix between HFB quasi-particle states and BCS quasi-particle states, as defined at p. 248 of Ref. [24]. The chemical potential difference $\lambda_n - \lambda_p$ is included in the energy denominator so that it can reproduce the RPA+PVC limit for magic nuclei, where the sign '+' is for T_- excitations and and '$-$' for T_+ excitations. The smearing parameter Δ is introduced to avoid singularities in the denominator, and a convenient practical value is $\Delta = 200$ keV. The detailed expression for $\langle a||V||a'', nL\rangle$ can be found in Ref. [22].

For nuclei not far from the stability line, like the nucleus ^{120}Sn studied in this work, the BCS quasi-particle states represent a convenient and accurate approximation to the HFB states. The corresponding expression for the spreading matrix elements is obtained by approximating the $C-$transformation with the identity, that is, putting $C_{a\tilde{a}''} = \delta_{a\tilde{a}''}$ in Eqs. (16-19). We checked this approximation in Fig. 1. We could see that this approximation is good for ^{120}Sn. More details of QRPA+QPVC formulas can be found in Ref. [22].

3 Results and Discussions

In this section, we will discuss the QPVC effects on GT response in ^{120}Sn. First of all, let's check the QPVC effects on Ikeda sum rule. The Ikeda sum rule tells us that the difference of total GT transition strength between T^- and T^+ channels is $3(N-Z)$. We use the Skyrme interaction SGII [25] in our calculation to check the Ikeda sum rule. In the QRPA calculation, 99.8% of the Ikeda sum rule is satisfied. In

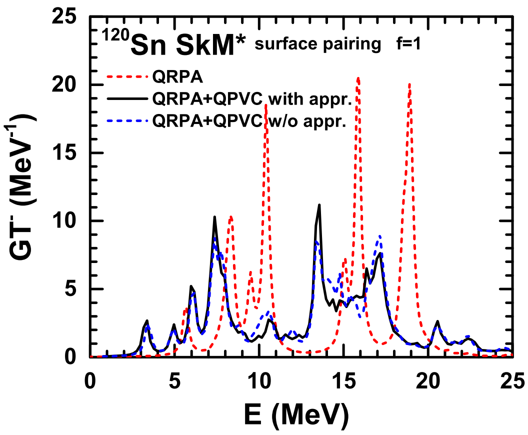

Figure 1: Gamow-Teller strength distribution in ^{120}Sn calculated by Skyrme QRPA+QPVC model with and without approximation in the spreading matrix elements, using Skyrme interaction SkM*.

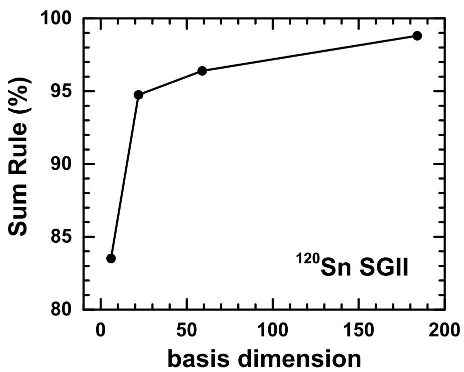

Figure 2: Ikeda sum rule fulfillment as a function of the number of QRPA basis states used for the QPVC calculation, in the case of the Gamow-Teller response of ^{120}Sn calculated with the interaction SGII. Taken from Ref. [22].

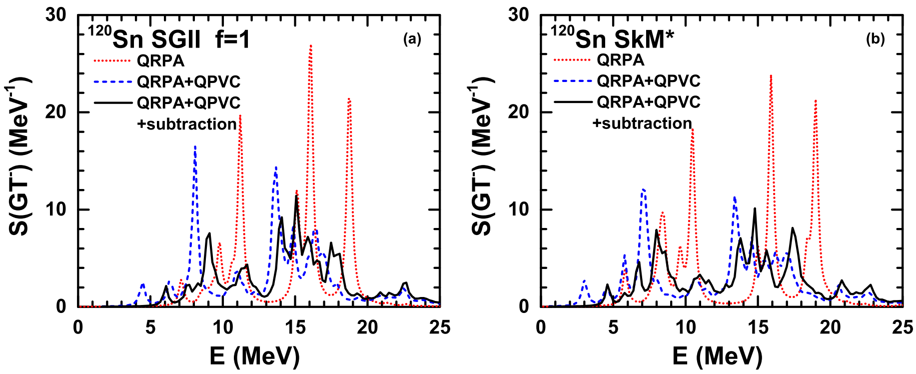

Figure 3: The Gamow-Teller strength distributions for ^{120}Sn calculated by means of QRPA, and QRPA+QPVC models without and with subtraction method, using the Skyrme interaction SGII [panel (a)] and SkM* [26] [panel (b)].

the QRPA+QPVC case, we plot in Fig. 2 the fulfillment of the Ikeda sum rule as a function of the number of QRPA basis states used for the QPVC calculation. In the QPVC calculation, Eq. (2.1) is solved in the QRPA basis. In order to simplify the calculation, we usually neglect QRPA states with very small GT strength, reducing significantly the dimension of the QRPA+QPVC matrix. The cutoff on the relative strength of the QRPA states is denoted as b_{cut}, namely only the QRPA states with a fraction of NEWSR strength larger than b_{cut} are included in the calculation. We check the sum rule as a function of the number of QRPA basis states obtained by setting $b_{cut} = 10^{-1}, 10^{-2}, 10^{-3}$ and 10^{-4}, in Fig. 2. We consider the integrated strength up to the excitation energy of 80 MeV. For $b_{cut} = 10^{-3}$, we obtain 97% of the Ikeda sum rule.

Another important issue in the QPVC calculation is the use of the so-called "subtraction" method. The subtraction method is introduced in order to avoid the double counting problem in the QPVC calculation, i.e., to make sure that the static effects beyond mean field absorbed in the parameters of the energy density functional are not considered again in the QPVC calculation [27, 28, 29, 30, 17].

Using the subtraction method, we correspondingly modify the QRPA + QPVC equation (2.1), by writing

$$\begin{pmatrix} \mathcal{D} + \mathcal{A}_1(E) - \mathcal{A}_1(0) & \mathcal{A}_2(E) - \mathcal{A}_2(0) \\ -\mathcal{A}_3(E) + \mathcal{A}_3(0) & -\mathcal{D} - \mathcal{A}_4(E) + \mathcal{A}_4(0) \end{pmatrix} \begin{pmatrix} F^{(\nu)} \\ \bar{F}^{(\nu)} \end{pmatrix} = $$
$$= (\Omega_\nu - i\frac{\Gamma_\nu}{2}) \begin{pmatrix} F^{(\nu)} \\ \bar{F}^{(\nu)} \end{pmatrix} \tag{3.1}$$

so that the above equation reduces to the QRPA equation when $E = 0$.

In Fig. 3, we plot the Gamow-Teller strength distributions for ^{120}Sn calculated by

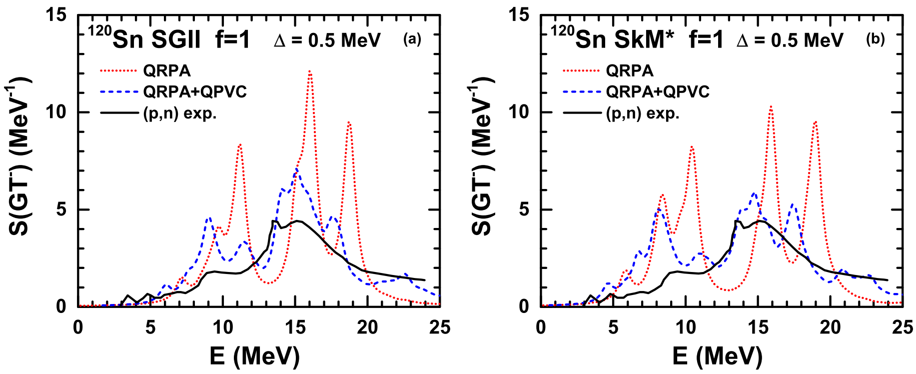

Figure 4: The Gamow-Teller strength distributions for ^{120}Sn calculated by QRPA and QRPA+QPVC models, using the Skyrme interaction SGII [panel (a)] and SkM* [panel (b)]. The smearing parameter $\Delta = 0.5$ MeV is used instead of $\Delta = 0.2$ MeV used for Fig. 3. The experimental results from (p,n) reactions are shown for comparison. The cross section from the (p,n) reaction is normalized by the unit cross section [31].

means of QRPA, and QRPA+QPVC models without and with subtraction method, using the Skyrme interaction SGII and SkM*. The effects of subtraction are quite similar for both interactions. With subtraction, the energies of GT excitations are shifted upwards as expected, going back to the QRPA results. The energy shift is more apparent at low energy regions, which is around 1 MeV, and becomes smaller with increasing excitation energy, which is around 0.5 MeV at the giant resonance region, until it almost vanishes at $E = 25$ MeV. With subtraction, the detailed fragmentations in both the low-energy region and the giant resonance region are modified. The centroid energies in the energy region $E = 0 - 25$ MeV are 14.6, 13.3, and 14.5 MeV for QRPA, QRPA+QPVC and QRPA+QPVC with subtraction calculation respectively for SGII interaction, while they are 13.9, 12.6, and 13.8 MeV for SkM* interaction. We could see that for both interactions, the centroid energy of QPVC result becomes almost the same as the QRPA result by using the subtraction method.

We compare our calculated Gamow-Teller strength distributions using the Skyrme interactions SGII and SkM* with experimental data in Fig. 4. We use a smearing parameter $\Delta = 0.5$ MeV in the QRPA and QRPA+QPVC calculation, instead of the value $\Delta = 0.2$ previously used in Fig. 3. This value corresponds to the energy resolution of the (p,n) experiment [31]. In Ref. [31], besides the cross section $\sigma(0^o)$, the unit cross section $\hat{\sigma} = 2.78 \pm 0.16$ mb/sr was also determined. We can then obtain an approximate value for the B(GT) strength by using the relation $\sigma(0^o) = \hat{\sigma} F(q, \omega) B(GT)$, and assuming that the factor $F(q, \omega)$, giving the dependence on momentum and energy transfer of the cross section, is constant and equal to 1. From QRPA to QRPA+QPVC, a much bigger width is developed for both interactions, and hence it gives a much better agreement with experimental data. In the giant resonance region, the experimental strength distribution is well reproduced, especially for SkM*. However, in the low energy region, the GT strength is overestimated by both interactions.

4 Conclusions

In this paper, the quasiparticle vibration coupling effects on GT response in ^{120}Sn are briefly discussed. In the QRPA+QPVC model, the Ikeda sum rule is still satisfied. The subtraction method is applied, and it shifts the excitation energy upwards, bringing the centroid energy of the QRPA+QPVC calculation, initially in the energy region $E = 0 - 25$ MeV, back to that of the QRPA model. Finally with the inclusion of QPVC, we can see that the data of GT response in the giant resonance region is well reproduced.

References

[1] F. Osterfeld, Rev. Mod. Phys. **64**, 491 (1992).

[2] K. Langanke, and G. Martinez-Pinedo, Rev. Mod. Phys. **75**, 819 (2003).

[3] H.-Th. Janka, K. Langanke, A. Marek, G. Martinez-Pinedo and B. Muller, Phys. Rep. **442**, 38 (2007).

[4] Z. M. Niu, Y. F. Niu, H. Z. Liang, W. H. Long, T. Niksic, D. Vretenar, and J. Meng, Phys. Lett. B **273**, 172 (2013).

[5] N. Paar, G. Colo‘, E. Khan, and D. Vretenar, Phys. Rev. C **80**, 055801 (2009).

[6] Y. F. Niu, N. Paar, D. Vretenar, and J. Meng, Phys. Rev. C **83**, 045807 (2011).

[7] N. Paar, D. Vretenar, T. Marketin, and P. Ring, Phys. Rev. C **77**,77, 024608 (2008).

[8] H. Z. Liang, Y. F. Niu, J. Meng, and N. Van Giai, J. Phys.: Conf. Ser. **267**, 012042, (2011).

[9] M. Ichimura, H. Sakai, and T. Wakasa, Prog. Part. Nucl. Phys. **56**, 446 (2006).

[10] Y. Fujita, B. Rubio, and W. Gelletly, Prog. Part. Nucl. Phys. **66**, 549 (2011).

[11] N. Paar, T. Niksic, D. Vretenar, and P. Ring, Phys. Rev. C **69**, 054303 (2004).

[12] Z. M. Niu, Y. F. Niu, H. Z. Liang, W. H. Long, and J. Meng Phys. Rev. C **95**, 044301 (2017).

[13] D. Gambacurta, M. Grasso, and F. Catara, Phys. Rev. C **81**, 054312 (2010).

[14] P. F. Bortignon, R. A. Broglia, D. R. Bes, and R. Liotta, Phys. Rep. **30**, 305 (1977).

[15] E. Litvinova, P. Ring, and V. Tselyaev, Phys. Rev. C **75**, 064308 (2007).

[16] E. Litvinova, P. Ring, and D. Vretenar, Phys. Lett. B **647**, 111 (2007).

[17] X. Roca-Maza, Y. F. Niu, G. Colo, and P. F. Bortignon, J. Phys. G: Nucl. Part. Phys. **44**, 044001 (2017).

[18] T. Marketin, E. Litvinova, D. Vretenar, and P. Ring, Phys. Lett. B **706**, 477 (2012).

[19] Y. F. Niu, G. Colo, M. Brenna, P. F. Bortignon, and J. Meng, Phys. Rev. C **85**, 034314 (2012).

[20] Y. F. Niu, G. Colo, and E. Vigezzi, Phys. Rev. C **90**, 054328 (2014).

[21] Y. F. Niu, Z. M. Niu, G. Colo, and E. Vigezzi, Phys. Rev. Lett. **114**, 142501 (2015).

[22] Y. F. Niu, G. Colo, E. Vigezzi, C. L. Bai, and H. Sagawa, Phys. Rev. C **94**, 064328 (2016).

[23] C. L. Bai, H. Sagawa, G. Colo, Y. Fujita, H. Q. Zhang, X. Z. Zhang, and F. R. Xu, Phys. Rev. C **90**, 054335 (2014).

[24] P. Ring and P. Schuck, *The Nuclear Many-Body Problem* (Springer-Verlag, Berlin, 1980).

[25] N. Van Giai and H. Sagawa, Phys. Lett. B **106**, 379 (1981).

[26] J. Bartel, P. Quentin, M. Brack, C. Guet, and H.-B. Hakansson, Nucl. Phys. A **386**, 79 (1982).

[27] K. Moghrabi, M. Grasso, G. Colo, and N. Van Giai, Phys. Rev. Lett. **105**, 262501 (2010).

[28] V. I. Tselyaev, Phys. Rev. C **75**, 024306 (2007).

[29] V. I. Tselyaev, Phys. Rev. C **88**, 054301 (2013).

[30] D. Gambacurta, M. Grasso, and J. Engel, Phys. Rev. C **92**, 034303 (2015).

[31] M. Sasano, H. Sakai, K. Yako, T. Wakasa, S. Asaji, K. Fujita, Y. Fujita, M. B. Greenfield, Y. Hagihara, K. Hatanaka et al., Phys. Rev. C **79**, 024602 (2009).